

ANALYSIS OF  $2\omega$  AND  $3\omega/2$  SPECTRA FROM PLASMAS PRODUCED BY  
IRRADIATION OF THIN FOIL TARGETS

A. Giulietti, D. Batani\*, V. Biancalana\*,  
D. Giulietti\*, L. Gizzi<sup>‡</sup>, L. Nocera and E. Schifano\*

Istituto di Fisica Atomica e Molecolare  
via del Giardino, 7, 56100, Pisa, Italy

\* Dipartimento di Fisica, Università' di Pisa, Italy

<sup>‡</sup> Imperial College, London, U.K.

ABSTRACT

Thin plastic foils have been irradiated at  $1.064 \mu\text{m}$  laser wavelength and an intensity up to  $5 \times 10^{13} \text{ W/cm}^2$ . The plasma produced became underdense during the laser pulse and electron temperatures of several hundred eV's were obtained. Second harmonic and three-halves harmonic emission have been studied perpendicularly to the laser beam axis. Time resolved imaging and spectroscopy gave us novel information on the physical mechanisms involved in these processes. The  $2\omega$  line was found to be red shifted consistently with the frequency sum between the incident laser light and the Brillouin backscattered radiation. Such an effect was already postulated to explain second harmonic side emission from filaments occurring in an underdense corona. However the occurrence of frequency sum in a plasma was demonstrated for the first time in our experiment.  $3\omega/2$  spectra showed an intense broadband red-shifted component and a very faint blue component. The analysis of spectral features of  $3\omega/2$  light, in terms of coupling between laser light and electron waves generated by Two Plasmon Decay (TPD) of the laser light itself, allowed us to conclude that the TPD plasmons propagate through the  $n_c/4$  layer before they couple.

I. INTRODUCTION

In the last years a lot of work has been done on the study of parametric instabilities developing in long scale length undercritical plasmas similar to those the laser radiation have to pass through before reaching the target denser regions in ICF experiments.<sup>(1,2)</sup>

Among the numerous plasma diagnostics, the detection and analysis of harmonics of laser radiation (both integer and half-integer) have been some of the most powerful<sup>(3-5)</sup>.

In particular  $3\omega/2$  radiation, detected at different angles, has been utilized to follow the motion of the quarter-critical layer ( $n_e \approx n_c/4$ ) and to measure electron temperature in the same region <sup>(6-13)</sup>. However the comparison between experimental results and theory was not always satisfactory. A complete understanding of the spectral features must take into account a number of possible contributions, including reflection of laser radiation inside the plasma and plasmon propagation<sup>(14)</sup> before they couple with laser radiation to produce  $3\omega/2$  harmonic.

The second harmonic has been mainly studied in presence of the critical density layer where its generation is by far more probable <sup>(15,16)</sup>. Only a few works report on the observation of  $2\omega$  emission from undercritical plasmas<sup>(17-19)</sup>. The mechanisms of  $2\omega$  generation and the information on plasma parameters that can be obtained are completely different in the two cases.

In the present experiment time resolved spectra and images at  $2\omega$  and  $3\omega/2$  were obtained at  $90^\circ$  to the beam axis from a plasma produced by laser irradiation of a thin plastic film. The plasma was underdense for most of the time of the laser pulse. To reduce sources of uncertainty in the analysis of the  $2\omega$  and  $3\omega/2$  spectra, we performed the experiment with a small aperture of the focusing and detection optics.

The analysis of  $2\omega$  spectra allowed us to confirm the hypothesis proposed by other authors <sup>(20)</sup> for the emission of second harmonic from an underdense plasma at  $90^\circ$  to the laser beam axis. On the other hand the  $3\omega/2$  spectra evidenced the relevance of the effect of propagation of plasmons created by Two Plasmon Decay (TPD), before they couple to generate  $3\omega/2$  radiation.

In section II we recall elements of the theory of  $3\omega/2$  and  $2\omega$  emission. The experimental apparatus is presented in section III. In section IV and V the experimental results are reported and discussed.

## II. THEORY

### Three-Halves Harmonic Generation

The  $3\omega/2$  radiation can be produced from both the coupling of the incident laser radiation with  $\omega/2$  plasma waves or the coalescence of three of those waves. However, as the three wave process is of higher order, coupling of laser radiation with plasma wave is expected to prevail in our experiment. Thus only the latter process will be considered.  $\omega/2$  plasmons can be produced close to  $n_c/4$  plasma density layer by TPD and Stimulated Raman Scattering (SRS); but, due to the lower threshold of the TPD as compared with SRS, only the former mechanism of plasmons production will be considered.

In TPD the laser ( $\omega_o, K_o$ ) and plasma ( $\omega_{B,R}, K_{B,R}$ ) waves satisfy the energy and momentum conditions:

$$\omega_o = \omega_B + \omega_R \quad (1)$$

$$\underline{K}_0 = \underline{K}_B + \underline{K}_R \quad (2)$$

which, with the dispersion relations for photons and plasmons, give the plasmon frequencies:

$$\omega_B \approx \omega_0/2 \left( 1 + 3/4 \left( K_B^2 - K_R^2 \right) \lambda_D^2 \right) \quad (3)$$

$$\omega_R \approx \omega_0/2 \left( 1 - 3/4 \left( K_B^2 - K_R^2 \right) \lambda_D^2 \right) \quad (4)$$

where  $\lambda_D$  is the Debye length.

With  $K_B > K_R$ , the plasmons ( $\omega_B, \underline{K}_B$ ), travelling with a wavevector component in the direction of the pump wave i.e.  $\underline{K}_0 \cdot \underline{K}_B > 0$  are blue shifted, while the plasmons ( $\omega_R, \underline{K}_R$ ), for which  $\underline{K}_0 \cdot \underline{K}_R$  can be positive or negative, are red shifted from the exact  $\omega_0/2$  frequency. In the following we will call them "blue" and "red" plasmons respectively.

In the most general case the plasmons from TPD propagate<sup>(14)</sup> through the inhomogeneous plasma before they couple with the pump photons. As a consequence the matching conditions for the  $3\omega/2$  emission process can considerably change in space, because in the quarter critical region the  $\underline{K}_{R,B}$  wavevectors dramatically depend on density. We consider here only density gradients parallel to  $\underline{K}_0$ , as those due to the target foil explosion. A perpendicular component of the density gradient is also usually present in laser produced plasmas due to the non-uniformity of illumination and eventually filamentation. This component can be shown to have a minor influence on  $3\omega/2$  spectra. On the contrary a gradient component perpendicular to  $\underline{K}_0$  is essential to generate second harmonic in underdense plasmas (see next subsection).

For laser radiation propagating along density gradient and coupling with TPD (red or blue) plasmons, the energy and momentum conservation for the process gives for the wavelength shift  $\Delta\lambda_{3/2}$  from exact  $2\lambda_0/3$  value:

$$\Delta\lambda_{3/2} = \lambda_0/2 \left( v_e/c \right)^2 \left[ 1 - (2\sigma/3)^{1/2} \right] \left( 11\alpha^2 \pm 4 \cdot 6^{1/2} \alpha^2 \cos\theta - 8\sin^2\theta \right)^{1/2} \quad (5)$$

Where  $v_e$  is the electron thermal velocity,  $\theta$  the angle between  $\underline{K}_0$  and  $\underline{K}_{3/2}$ ,  $\sigma = (\underline{K}_0 \cdot \underline{K}_{B,R}) / |\underline{K}_0 \cdot \underline{K}_{B,R}|$  and  $\alpha = |\underline{K}_{B,R}| / |\underline{K}'_{B,R}|$ ,  $\underline{K}_{B,R}$  and  $\underline{K}'_{B,R}$  being the wavevector of the plasmon before and after its propagation respectively. Notice that the "-" sign refers to incident laser light ( $\omega_0, \underline{K}_0$ ) and the "+" sign to backpropagating light ( $\omega_0, -\underline{K}_0$ ). As it is evident from the equation (5) the plasmon propagation results in an additional shift of  $3\omega/2$  radiation, the ordinary shift being an effect of the plasma temperature. Because a range of different  $\alpha$ 's is allowed the plasmon propagation is a source of  $3\omega/2$  line broadening as well.

It is important to note that the measurements of  $3\omega/2$  spectrum can give an estimation of electron temperature in the  $n_c/4$  region, but the propagation of plasmons makes this diagnostic less accurate due to the variability of  $\alpha$ .

## Second Harmonic Generation from Underdense Plasmas

Close to the critical density different mechanisms developing during the laser-plasma interaction can produce  $2\omega$  radiation. In fact in this region  $\omega_0$  plasmons can be generated either by resonant absorption or Electron Ion Decay. Such plasmons interacting in couples or with another pump photon can easily produce  $2\omega$  radiation at different angles<sup>(21)</sup>. There is also another way to produce  $2\omega$  radiation that consists in the interaction of the impinging electromagnetic wave with density gradients inside the plasma<sup>(22)</sup>.

The last mechanism is the only one that can still work in underdense plasmas; but, due to the radial symmetry typical of laser produced plasmas, it provides a forward emission of  $2\omega$  radiation in a small angle from the laser beam axis<sup>(18,23)</sup>.  $2\omega$  radiation from underdense plasmas was detected at  $90^\circ$  only in few experiments. In one of them  $2\omega$  radiation at  $90^\circ$  was used to image filaments created in an underdense plasma. The authors<sup>(20)</sup> proposed a theory to explain such an emission as a result of the interaction of the impinging laser radiation with backreflected radiation at about the same frequency, in presence of density gradients in the plasma. According to the theory, the  $2\omega$  emission originates from the current density

$$\mathbf{j}_{2\omega} = (e^3/2im^2\omega^3) [\underline{E}_0 \underline{E}_0 e^{2iK_0 z} + \underline{E}_B \underline{E}_B e^{-2iK_0 z} + (\underline{E}_0 \underline{E}_B + \underline{E}_B \underline{E}_0)] \cdot \nabla n \quad (6)$$

where  $\underline{E}_0$  and  $\underline{E}_B$  are the amplitudes of electric fields of impinging and backreflected laser radiation and  $\nabla n$  represents the density gradients in the plasma. The equation (6) shows that a radial component for  $\nabla n$  is needed to allow  $2\omega$  emission.

This component is usually present in laser produced plasmas, in case enhanced by self-focusing and filamentation of the laser beam. As one can verify the first term contributes only for small angles ( $\gamma \sim 0$ ) in an angular width  $\Delta\gamma \sim (2\lambda/l_F)^{1/2}$ ;  $\gamma$  being the angle between the laser beam axis ( $z$ ) and the direction of observation, and  $l_F$  the length of the emitting region.

The second term is responsible for the  $2\omega$  backscattered radiation, contributing for  $\gamma \sim \pi$ , while the third contributes only for  $\gamma \sim \pi/2$  in an angular width  $\Delta\gamma \sim \lambda/l_F$ .

### III. EXPERIMENTAL SETUP

The experimental setup is shown in Fig.1. A Nd laser ( $\lambda_0 = 1.064 \mu\text{m}$ , spectral width  $\Delta\lambda \approx 0.7 \text{ \AA}$ ), delivering up to 3 J in 3 nsec (FWHM), was focused on target by an  $f/8$  lens into a vacuum chamber. In a  $60 \mu\text{m}$  diameter focal spot an intensity up to  $5 \times 10^{13} \text{ W/cm}^2$  was reached. Time modulations were present into the pulse, due to beating of longitudinal modes. Prepulse level was kept below  $10^{-4}$  the main pulse and it was experimentally checked that this level could not produce any early plasma formation. This was not the case for a small number of shots for which the interaction showed completely different character.

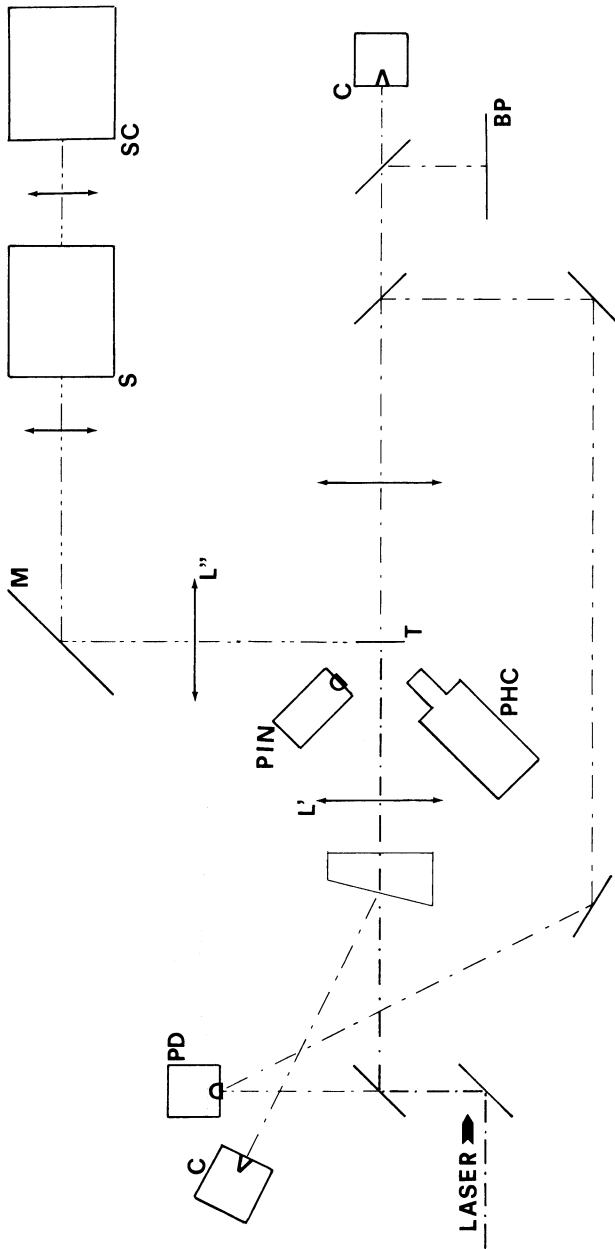


Fig. 1. Experimental set-up. C - calorimeter; PD - photodiode; BP - burn paper; L'- focusing lens; T - target; PIN - X-ray diode; PHC - pin-hole camera; L'' - collecting lens; S - spectrometer; SC - streak camera. The spectrometer was replaced by a narrowband filter to obtain time resolved images of the harmonic sources.

The targets used consisted of thin formvar foils (polyvinyl formal  $[C_5 H_{11} O_2]$  ; density = 1.1 g/cm<sup>3</sup> ;  $Z_a \approx 3$ ) , whose thickness ranged from 0.1  $\mu\text{m}$  to 1.6  $\mu\text{m}$  and was measured with an interferometric method <sup>(24)</sup>. The target was irradiated at normal incidence and the laser light was linearly polarized at 45° with respect to the irradiation/detection plane.

The radiation was collected at 90° from the beam axis, using an f/7 optics, and imaged into the entrance slit of a spectrometer coupled with a Hadland streak camera. The overall spectral resolution resulted 3 Å and the time resolution was 20 ps. The collecting optics was designed in order to have no spatial selection of the  $3\omega/2$  and  $2\omega$  sources. Spectral calibration was performed with the 7032 Å, 7174 Å, 7245 Å lines of Ne for the  $3\omega/2$  spectra and 5330 Å, 5341 Å, 5400 Å lines of Ne for the  $2\omega$  spectra. A wavelength fiducial was obtained putting a thin wire on the spectrometer output plane, perpendicularly to the dispersion axis. The position of the wire was in turn calibrated with the same spectral lines.

Alternatively, to obtain the time resolved images of the emitting regions, the spectrometer was replaced with a narrow band filter (100 Å FWHM centered at 7090 Å for the  $3\omega/2$  and 30 Å FWHM at 5320 Å for the  $2\omega$  spectra) and the interaction region imaged directly into the entrance slit of the streak-camera, with a magnification  $G \approx 10$ . The streak-camera slit was superimposed to the laser beam axis in the image of the plasma. The slit aperture was set in order to match the focal spot diameter and the spot image was carefully positioned. This set-up allowed to localize the position of the  $3\omega/2$  and  $2\omega$  sources along the interaction region.

#### IV. EXPERIMENTAL RESULTS

In Fig.2 a spectrum, obtained at low dispersion, shows both  $3\omega/2$  and  $2\omega$  lines. Together with the two harmonics the bremsstrahlung emission is apparent.

In Fig.3 and Fig.4 the spectra of the two harmonics, obtained at higher dispersion, are reported; Fig.5 and Fig.6 show the images of the sources of the two harmonics. A time modulation of the emission, resulting in spikes of tens of picoseconds is apparent. It is due to the intensity modulation already present in the laser pulse. The wavelength fiducial looks like an artificial intensity minimum in the two spectra. The dashed line parallel to the time-axis shows the position of the exact  $3\omega_0/2$  and  $2\omega_0$  lines respectively. It is interesting to observe that, while the  $3\omega/2$  radiation was characterized by well defined regions of emission and a broad spectrum, the  $2\omega$  radiation was emitted from wide plasma regions with a narrow spectrum. This is an indication of completely different mechanisms of emission for the two cases. In fact  $3\omega/2$  radiation can be emitted only in a density region close to  $n_c/4$  via the interaction of e.m. waves with plasmons of broad energy spectrum. On the other hand  $2\omega$  radiation is generated at 90° by the interaction of two counterpropagating e.m. waves of about the same bandwidth as the laser light; this process can take place virtually in the whole laser plasma interaction volume.

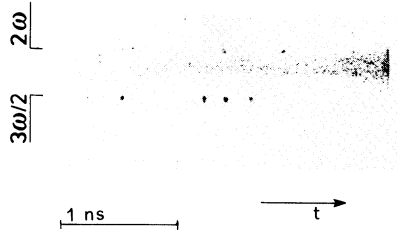


Fig.2. Low dispersion time resolved spectrum of light collected perpendicularly to the beam axis. Shot #061204; formvar foil thickness =  $1.34 \mu\text{m}$ ; laser irradiance  $I = 1.3 \times 10^{13} \text{ W/cm}^2$ . Second harmonic and  $3/2$  harmonic of the laser light are visible as isolated spikes. Continuum plasma emission is also shown as background more intense in the yellow-green region of the spectrum because of cathode sensitivity of the streak camera.  $3\omega/2$  emission is much more intense than  $2\omega$  one. Only few spikes show coincidence of two emissions, due to the completely different mechanism of their generation.

The laser intensity threshold to generate  $3\omega/2$  light resulted  $I_{\text{th}} \approx 5 \times 10^{12} \text{ W/cm}^2$ , but this harmonic completely disappeared in case of prepulse level higher than  $10^{-4}$  the main pulse. This is due to the fact that, in such a condition, the plasma is produced earlier and the electron density is lower than  $n_c/4$  at the time of the main pulse.  $3\omega/2$  spectra showed a strong variability from one spike to another, either for what concerns shift and width. However all the spectra were red shifted even if some of them showed a faint blue component too.

From the images like that reported in Fig.6 we estimated the scalelength of the density gradients in the  $n_c/4$  region. We found values of a few tens of micrometers, which reasonably agree with the London-Rosen expansion model <sup>(25)</sup>.

Spatial modulations along the laser beam axis can be observed in most of spikes in the  $2\omega$  images.

## V. DISCUSSION AND CONCLUSION

The spectra of  $3\omega/2$  light emitted at  $90^\circ$  we obtained are characterized by considerable values of both red shift and bandwidth. Such values are very difficult to explain if the propagation of TPD plasmons is not considered. As matter of fact in this case both temperature and Doppler effects give shifts lower than the mean shift of  $\approx 35 \text{ \AA}$  we observed on a large number of shots.

More pronounced is the discrepancy for the  $3\omega/2$  bandwidth.

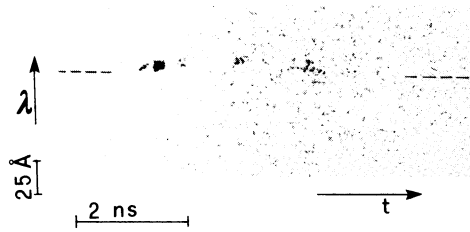


Fig. 3. Time resolved spectrum of  $2\omega$  emitted at  $90^\circ$ .  
 Shot #231203;  $d = 1.50 \mu\text{m}$ ;  $I = 1.1 \times 10^{13} \text{ W/cm}^2$ .  
 The dashed line matches the exact  $\lambda_0/2$  wavelength.

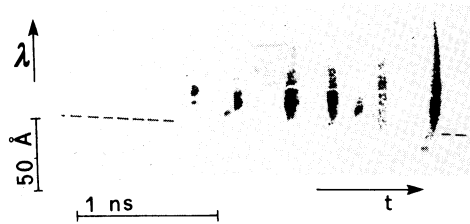


Fig. 4. Time resolved spectrum of  $3\omega/2$  emitted at  $90^\circ$ .  
 Shot #191202;  $d = 1.50 \mu\text{m}$ ;  $I = 1.0 \times 10^{13} \text{ W/cm}^2$ .  
 The dashed line matches the exact  $2\lambda_0/3$  wavelength.



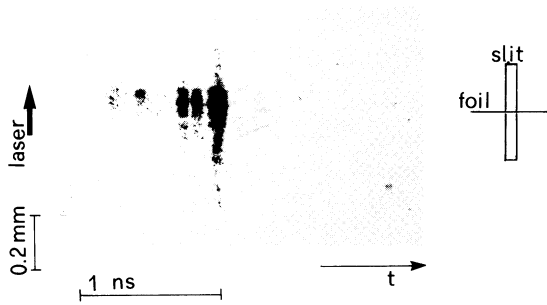


Fig. 5. Time resolved image of  $2\omega$  emitting sources taken at  $90^\circ$  to the laser beam axis. Shot #060204;  $d = 1.39 \mu\text{m}$ ;  $I = 1.5 \times 10^{13} \text{ W/cm}^2$ . The relative position of foil target, laser beam and streak camera slit is shown.

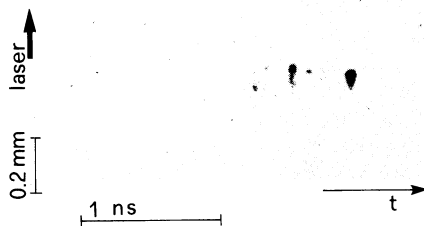


Fig. 6. Time resolved image of  $3\omega/2$  emitting sources taken at  $90^\circ$  to the laser beam axis. Shot #020204;  $d = 0.8 \mu\text{m}$ ;  $I = 1.1 \times 10^{13} \text{ W/cm}^2$ .

In fact in case of non-propagation we can take into account several causes of line broadening. The broadening due to Landau damping is negligible in our experimental conditions for  $3\omega/2$  observed at  $90^\circ$ . Let us consider collisional broadening. The electron-ion collision frequency is related to the damping coefficient  $\Gamma_c$  of a plasma wave (of complex frequency  $\omega$ ) by the relation

$$\Gamma_c = \text{Im}(\omega) = v_{ei}/2 \quad .$$

In our conditions

$$v_{ei} \approx 6.7 \times 10^{-11} (Z n_e \ln \Lambda T_e^{-3/2}) \approx 2 \times 10^{12} \text{ sec}^{-1}$$

and the collisional width is  $\delta\omega = v_{ei}$ , giving  $\delta\lambda_c \approx 5 \text{ \AA}$ .

Finally the effect of the aperture of focusing ( $\Theta_f \approx 8^\circ$ ) and collecting ( $\Theta_c \approx 7^\circ$ ) optics results in an overall instrumental width  $\Delta\lambda_{\text{aper}} \approx 3 \text{ \AA}$ .

Due to the effects considered above, the  $3\omega/2$  line can be broadened of a few  $\text{\AA}$ , a small extent if compared with the observed bandwidth of several tens of  $\text{\AA}$ . We believe that the observed shift and broadening of the  $3/2$  harmonic in this experiment are a clear evidence of the propagation of the electron waves through an inhomogeneous plasma.

From the analysis of Sect. II we know that the  $3\omega/2$  radiation we detected at  $90^\circ$  is mostly a "direct" emission produced by coupling of the impinging laser radiation with red plasmons ( $\omega_R, K_R$ ). However we will consider also the "indirect" emission which can be given by the coupling of  $\omega/2$  plasmons reflected at the  $n_c/4$  layer. In this case we intend with reflection a particular case of propagation, able to invert the component of the plasmon momentum along  $K_o$ . Moreover, as in this experiment we evidenced a small amount of Brillouin scattering, we can not exclude the presence of a very weak "indirect" line from the coupling of SBS backscattered photons ( $\omega_o, -K_o$ ) with blue plasmons ( $\omega_B, K_B$ ). The blue component of the  $3/2$  harmonic is usually absent in our spectra, or very weak in a few spikes. This is not surprising because: i) the contribution of photons reflected at the critical layer is small (the plasma becoming underdense before the  $n_c/4$  layer develops to suitable scalelength), ii) the intensity of Brillouin backscattered light is very weak, as already mentioned. On the other hand the lack of a significant blue component also means that the reflection of  $\omega/2$  plasmons propagating in the  $n_c/4$  region is not an efficient process.

Finally some considerations about the threshold. We observed a threshold for 3/2 harmonic emission at nominal laser intensity of  $5 \times 10^{12} \text{ W/cm}^2$ . This value is much lower than the expected threshold for TPD. Considering an  $n_c/4$  layer scalelength of  $30 \mu\text{m}$ , which is a mean value of measurements taken from time resolved images, we find that the TPD threshold is dominated by plasma inhomogeneities and its value can be estimated of the order of  $10^{14} \text{ W/cm}^2$ . It is very reasonable that the discrepancy between the measured and calculated values of the threshold is due to the presence of hot spots and filaments into the interaction region which can lead to a local increase of the laser field. This point demands further experimental study to be clarified.

For what concerns the  $2\omega$  spectroscopic data, they are consistent with second-harmonic emission resulting from the sum of the laser frequency with the frequency of Brillouin backscattered light. The measured threshold of the  $2\omega$  emission agrees with the expected SBS threshold in our experimental condition. The main signature of this process comes from the red shift of the backscattered light as expected from SBS which in turn gives a red shift of the second-harmonic light. The frequency of  $2\omega$  field is exactly  $\omega_o + \omega_B$  where  $\omega_B$  is the frequency of the Brillouin backscattered wave, given by

$$\omega = \omega_o [1 - 2v_i/c [ (1-n_e/n_c) / (1+4K_o^2 \lambda_D^2 (n_c/n_e - 1) ) ]^{1/2}] \quad (7)$$

where  $v_i = [(ZT_e + 3T_i)/m_i]^{1/2}$  is the speed of the ion acoustic wave,  $T_e$  and  $T_i$  are the electron and ion temperature, respectively, in energy units. Our data are consistent with this explanation provided one takes into account that

$$\Delta\omega/\omega \Big|_{2\omega_o} = 1/2 \Delta\omega/\omega \Big|_{\omega_o} \quad (8)$$

The initial position of the  $2\omega$  line has a red shift  $\Delta\lambda \approx 4 \text{ \AA}$  corresponding to  $v_i = 2.5 \times 10^7 \text{ cm sec}^{-1}$ , i.e.,  $T_e \approx T_i \approx 600 \text{ eV}$ . This temperature, roughly constant in time after burnthrough, i.e., during the peak of the laser pulse, is expected<sup>(25)</sup> in the given experimental condition when  $2\omega$  light is mostly emitted.

The increase in red shift observed during the emission is explainable in terms of Doppler shift due to the plasma motion in the direction of the beam axis (parallel to  $K_o$ ). This motion is accelerated due to ablation pressure. From the red shift at  $2\omega$  the velocity  $v_p$  of the plasma motion can be evaluated if we put in equation (7)  $v_i + v_p$  in place of  $v_i$ , taking  $v_i = 2.5 \times 10^7 \text{ cm sec}^{-1}$ .

For all the spectra obtained with  $1-1.5 \mu\text{m}$  targets we find  $v_p \approx 2 \times 10^7 \text{ cm sec}^{-1}$  at delays of a few hundred picoseconds, up to  $v_p \approx 6 \times 10^7 \text{ cm sec}^{-1}$  after  $\approx 2 \text{ ns}$ . These velocities are reasonable in our experimental condition and are comparable with direct measurements performed by other authors<sup>(26)</sup>.

The  $2\omega$  line bandwidth showed a net increase during the emission, typical from  $5 \text{ \AA}$  to about  $20 \text{ \AA}$ . It is a consequence of the increasing bandwidth of the electromagnetic wave backscattered by the Brillouin process. Landau damping of ion sound waves could be in principle responsible for line

broadening, but calculation leads to a narrower bandwidth than observed. We believe that the line bandwidth is essentially due to Doppler broadening related to plasma expansion. Consequently, the doublet structure apparent in most late-time spikes should indicate that two plasma regions with different velocities are more effective in SBS (and consequently in sum-frequency generation).

The frequency sum process, postulated by Stamper et al.<sup>(20)</sup> is now experimentally confirmed<sup>(27)</sup> as a nonlinear process occurring in laser-produced plasmas as well as already observed in crystals<sup>(22)</sup>.

Finally let us consider the implications of our study of harmonic emission at  $90^\circ$  from the point of view of laser produced plasma diagnostics. Spectroscopy of  $2\omega$  light generated by sum frequency has in principle the same diagnostic power than the spectroscopy of Brillouin backscattered light. This latter is commonly used to measure electron temperature, estimate plasma turbulence and related parameters. Sum frequency light can give the same sort of information with the net experimental advantages of a larger spectral separation and a comfortable angle of detection (perpendicular to the laser beam).

The diagnostic use of  $3\omega/2$  light is first of all in localizing the  $n_c/4$  layer and measure its scalelength. The shift of this harmonic from the  $3\omega_0/2$  exact value can be used to measure the plasma temperature. The linear dependence of the shift on temperature makes these measurements very efficient. But from our experimental observations we realized that the propagation of the plasmons can modify the shift and strongly increase the broadening of the  $3\omega/2$  line, resulting in a poor accuracy of temperature measurements.

Several features of  $2\omega$  and  $3\omega/2$  spectra obtained in this experiment can be related to the influence of filamentation on the generation of these harmonics. Further studies could allow to use  $2\omega$  and  $3\omega/2$  spectroscopy as a diagnostic of filamentation itself.

#### ACKNOWLEDGEMENTS

Thanks are due to I. Deha for valuable contributions and to S. Bartalini for his creative technical support. We are also grateful to the target preparation group of the Laser Division of Rutherford Appleton Laboratory (UK) for the information on thin foil target fabrication.

The experiment was fully supported by Consiglio Nazionale delle Ricerche, Italy.

#### REFERENCES

- 1) R.P. Drake, E.A. Williams, P.E. Young, K. Estabrook, W.L. Kruer, H.A. Baldis and T.W. Johnston, *Phys. Rev. Lett.* **60**, 1018, (1988).
- 2) O. Willi, D. Basset, A. Giulietti and S.J. Karttunen, *Opt. Comm.*, **70**, 487, (1989).
- 3) V. Yu. Bychenkov, V.P. Silin and V. T. Tikhonchuk, *Sov. J. Plasma Phys.* **3**, 730 (1977).

- 4) W. Seka, B.B. Afeyan, R. Boni, L.M. Goldman, R.W. Short, K.Tanaka and T. W. Johnston, *Phys. Fluids* **28**, 2570 (1985).
- 5) N.G. Basov, Yu. A. Zadharenkov, N.N. Zorev, A.A. Rupasov, G.V.Sklizkov, A.S. Shikanov, in *Heating and compression of thermonuclear targets by laser beam*, edited by N.G. Basov (Cambridge University Press, 1986), and references therein.
- 6) S. Jackel, B. Perry and L. Lubin, *Phys. Rev. Lett.* **37**, 95 (1976).
- 7) Lin Zunqi, Tan Weihan, Gu Min, Mei Guang, Pan Chengming, Yu Wenyan and Deng Ximing, *Las. Part. Beams* **4**, 223 (1985).
- 8) T.A. Leonard and R. A. Cover, *J. Appl. Phys.* **50**, 3241 (1979).
- 9) P. D. Carter, S. M. L. Sim, H. C. Barr and R. G. Evans, *Phys. Rev. Lett.* **44**, 1407 (1980).
- 10) E. McGoldrick and S. M. L. Sim, *Opt. Comm.* **39**, 172 (1981).
- 11) L. V. Powers and R. J. Schroeder, *Phys. Rev. A* **29**, 2298 (1984).
- 12) V. Aboites, T. P. Hughes, E. McGoldrick, S. M. L. Sim, S. J. Karttunen and R. G. Evans, *Phys. Fluids* **28**, 2555 (1985).
- 13) F. Amiranoff, F. Briand and C. Labaune, *Phys. Fluids* **30**, 2221 (1987).
- 14) S.J. Karttunen, *Laser and particle beams* **3**, 157 (1985).
- 15) H.J. Herbst, J.A. Stamper, R.R. Whitlock, R.H. Lehberg, and B.H. Ripin, *Phys. Rev. Lett.*, **46**, 328, (1981).
- 16) N.G. Basov, V.Yu. Bychenkov, O.N. Krokhin, M.V. Osipov, A.A. Rupasov, V.P. Silin, G.V. Sklizkov, A.N. Starodub, V.T. Tikhonchuk, and A.S. Shikanov, *Sov. Phys. JETP*, **49**(6), (1979).
- 17) I.V. Alexandrova et al., *Pis'ma Zh. Eksp. Teor. Fiz.*, **38**, 478, (1983); [*JETP Lett.*, **38**, 577, (1983)].
- 18) D. Giulietti, G.P. Banfi, I. Deha, A. Giulietti, M. Lucchesi, L. Nocera, and Chen Zezun, *Laser and Particle Beams*, **6**, 141, (1988).
- 19) D. Batani, F. Bianconi, A. Giulietti, D. Giulietti, and L. Nocera, *Opt. Comm.* **70**, 38, (1989).
- 20) J.A. Stamper, R.H. Lehberg, A. Schmitt, M.J. Herbst, F.C. Young, J. H. Gardner, and S. P. Obenschain, *Phys. Fluids*, **28**, 2563, (1985).
- 21) Gu Min and Tan Weihan, *Laser and Particle Beams*, **6**, 569, (1988).
- 22) Y.R. Shen, *The Principles of Non linear Optics*, (Wiley, New York, 1984).
- 23) A. Giulietti, D. Giulietti, L. Nocera, I. Deha, Chen Zezun, and G.P. Banfi, *Laser Interaction*, **8**, 365, (1988).
- 24) Z. Z. Chen and E. Schifano, *IFAM Internal Report*, Jan. 1988.
- 25) R.A. London and M.D. Rosen, *Phys. Fluids* **29**, 3813 (1986).
- 26) K. Eidman, F. Amiranoff, R. Fedosejevs, A.G.M. Maaswinkel, R. Petsch, R. Sigel, G. Spindler, Yung-lu Teng, G. Tsakiris, and S. Witkowski, *Phys. Rev.*, **A 30**, 2568, (1984).
- 27) A. Giulietti, D. Giulietti, D. Batani, V. Biancalana, L. Gizzi, L. Nocera and E. Schifano, *Phys. Rev. Lett.*, **63**, 524 (1989).